JACS
JOURNAL OF THE AMERICAN CHEMICAL SOCIETY

Article

pubs.acs.org/JACS

Biomimetic Design Results in a Potent Allosteric Inhibitor of Dihydrodipicolinate Synthase from *Campylobacter jejuni*

Yulia V. Skovpen, Cuylar J. T. Conly, David A. R. Sanders,* and David R. J. Palmer*

Department of Chemistry, University of Saskatchewan, 110 Science Place, Saskatoon, Saskatchewan, Canada S7N 5C9

Supporting Information

ABSTRACT: Dihydrodipicolinate synthase (DHDPS), an enzyme required for bacterial peptidoglycan biosynthesis, catalyzes the condensation of pyruvate and β-aspartate semialdehyde (ASA) to form a cyclic product which dehydrates to form dihydrodipicolinate. DHDPS has, for several years, been considered a putative target for novel antibiotics. We have designed the first potent inhibitor of this enzyme by mimicking its natural allosteric regulation by lysine, and obtained a crystal structure of the protein-inhibitor complex at 2.2 Å resolution. This novel inhibitor, which we named "bislysine", resembles two lysine molecules linked by an ethylene bridge between the α-carbon atoms. Bislysine is a mixed partial inhibitor with respect to the first substrate, pyruvate, and a noncompetitive partial inhibitor with respect to ASA, and binds to all forms of the enzyme with a K_i near 200 nM, more than 300 times more tightly than lysine. Hill plots show that the inhibition is cooperative, indicating that the allosteric sites are not independent despite being located on opposite sides of the protein tetramer, separated by approximately 50 Å. A mutant enzyme resistant to lysine inhibition, Y110F, is strongly inhibited by this novel inhibitor, suggesting this may be a promising strategy for antibiotic development.

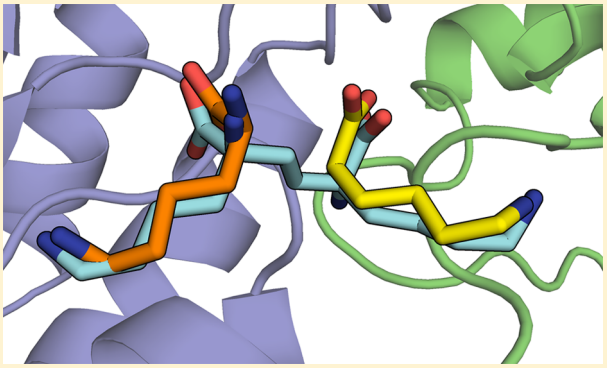

INTRODUCTION

The need for novel antibiotics is well-documented; in particular, there has been a striking lack of new drugs for Gram-negative bacteria in the last three decades.[1] Dihydrodipicolinate synthase (DHDPS) is considered a target for new antibiotics due to its essential role in the diaminopimelate (dap) pathway responsible for biosynthesis of *meso*-diaminopimelate and L-lysine, required components of the cell wall peptidoglycan.[2,3] The chemical and kinetic mechanisms of DHDPS are well-described: DHDPS is a Schiff-base-dependent aldolase catalyzing the conversion of pyruvate and (*S*)-aspartate-β-semialdehyde (ASA) to (4*S*)-hydroxy-2,3,4,5-tetrahydro-(2*S*)-dipicolinate, which spontaneously dehydrates to dihydrodipicolinate (Figure 1).[4] The reaction follows classical ping-pong kinetics, with pyruvate required to bind and form a Schiff base with an active-site lysine before ASA binds and reacts.[4,5] Despite this knowledge, inhibitors designed to target the active site of DHDPS have not yielded promising results,[6−9] and it has not been demonstrated that this enzyme can be inhibited effectively. Here we report that potent inhibition is possible, by mimicking the natural regulation mechanism.

DHDPSs from Gram-negative bacteria are regulated by the end-product of the dap pathway, L-lysine, by allosteric binding at low concentrations of inhibitor. The DHDPS from *Campylobacter jejuni* (*Cj*DHDPS), for example, is inhibited with an apparent IC_{50} of 65 μM.[5] Complete analysis shows the inhibition behavior to be complex: lysine is an uncompetitive partial inhibitor with respect to the first substrate, pyruvate, and a mixed partial inhibitor with respect to ASA. The partial inhibition means that ∼10% of the activity remains at saturating concentrations of lysine. The inhibition is also highly cooperative.

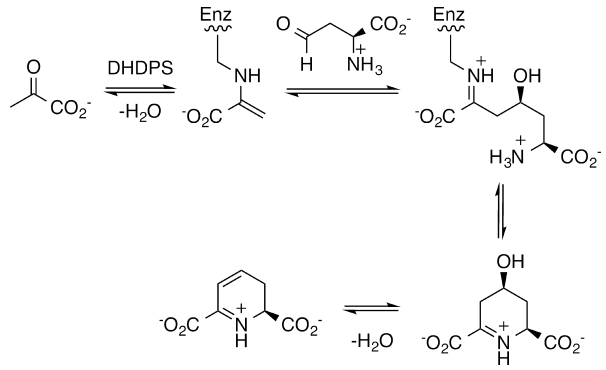

Figure 1. Reaction catalyzed by DHDPS. Pyruvate condenses with Lys166 prior to binding by ASA and subsequent aldol reaction.

Structural studies help explain the observed cooperativity. DHDPS from Gram-negative bacteria (and many Gram-positives) are homotetrameric, and can be described as a loose dimer of tight dimers. At the tight dimer interface, an allosteric cavity binds two lysine molecules with their α-carbon

Received: December 4, 2015
Published: February 2, 2016

DOI: 10.1021/jacs.5b12695
J. Am. Chem. Soc. 2016, 138, 2014−2020

atoms ~4 Å apart. Binding of one lysine molecule understandably affects binding of the adjacent molecule, and this is supported by isothermal titration calorimetry.[10,11] Notably, Hill coefficients for inhibition of *Cj*DHDPS by lysine exceed 2, suggesting that binding to one allosteric site affects the antipodal allosteric site.[5] Indeed, inhibition is thought to result in part from altered protein motions throughout the tetrameric structure.[12−14]

We hypothesized[10] that design of a molecule that would mimic two lysine molecules would be the most effective route to a potent inhibitor. By making a single inhibitor molecule that could occupy the allosteric site, a significant entropic advantage can be gained by eliminating the second binding event. Examination of crystal structures suggested that connecting the α-carbon atoms with a two-carbon linker would result in the closest biomimetic structure. Here we describe the synthesis of that molecule, which we have named "bislysine" (Figure 2), the

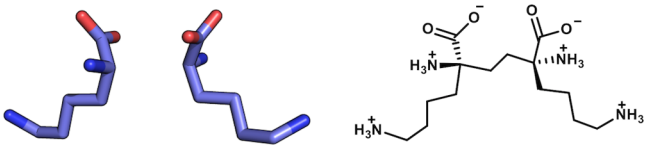

Figure 2. Binding mode of two L-lysine molecules in the allosteric site as shown by X-ray crystallography (PDB code 4M19) (left); the basis for the design (*R*,*R*)-bislysine (right).

kinetics of inhibition, and the high-resolution crystal structure of *Cj*DHDPS bound to bislysine and pyruvate. We have also performed similar studies with an allosteric site mutant, Y110F, which we have shown previously to be nearly insensitive to lysine inhibition.[14]

EXPERIMENTAL PROCEDURES

Preparation of bislysine. Synthesis and characterization of bislysine and its precursors are described in the Supporting Information. HPLC separations were performed on an Agilent 1100 series instrument consisting of a quaternary pump, autosampler, diode array detector (DAD) and evaporative light scattering detector (ELSD). A chiral semipreparative Astec CHIROBIOTIC T column (25 cm × 10.0 mm, Supelco Analytical) was used for separation of enantiomers. Ammonium acetate buffer (250 mM, pH 4.5) with 70% methanol was used as a mobile phase for separation of the protected racemic mixture and deprotected individual stereoisomers. The mobile phase was degassed by sparging with helium for 20 min. Instrument parameters were set to the following: flow rate, 2.0 mL/min; injection volume, 25 μL; DAD, 254 nm; ELSD temperature, 50 °C; ELSD gain, 5. Acquisition and processing of data was done using ChemStation LC Software (Rev.B.04.02; Agilent Technologies Inc.). All experiments were performed isocratically. The column was initially washed with methanol and equilibrated with the mobile phase for 30 min. For quantitative separations, a 7.3 mg/mL solution of a phthalimide-containing methyl ester precursor (Supporting Information, compound **9**) of bislysine was prepared in methanol (Supporting Information Figure 2). Only the DAD detector was used for runs involving fraction collection. The middle fraction between peaks of enantiomers was discarded to avoid cross-contamination. Fractions of each enantiomer were combined and evaporated under reduced pressure and moderate heating (40 °C) to remove all ammonium acetate. The ^{1}H NMR spectrum of each sample was collected to confirm that ammonium acetate had been removed. Each enantiomer obtained was hydrolyzed and purified on a cation exchange column as described in the Supporting Information. The purity of each enantiomer was judged by HPLC. The 8.6 mg/mL solutions of (*R*,*R*)- and (*S*,*S*)-bislysine were prepared in water and analyzed using the same HPLC method as for protected precursor **9**. Each enantiomer was tested as an inhibitor of DHDPS. The active enantiomer was presumed to be the (*R*,*R*)-isomer, later confirmed by protein crystallography.

Enzymology. *Expression and purification of DHDPS and dihydrodipicolinate reductase (DHDPR).* Expression and purification of DHDPS and DHDPR from *C. jejuni* have been described.[5] The obtained proteins were concentrated to 0.37 mg/mL for DHDPS and 1.29 mg/mL for DHDPR.

Enzyme assays and inhibition studies. The initial velocity of the DHDPS enzymatic reaction was determined in a coupled assay by monitoring the decrease in absorbance at 340 nm due to oxidation of NADH (ε_{340} = 6220 $M^{-1}cm^{-1}$) as described previously.[5] All kinetic measurements were made in 100 mM HEPES buffer at pH 8.0. A one-mL assay contained 0.16 mM NADH, 0.37 μg of DHDPS, 7.15 μg DHDPR and varying concentrations of ASA (0.066−2.6 mM) and pyruvate (0.20−3.7 mM). A 0.0084 mM solution of (*R*,*R*)-bislysine (tetrahydrobromide salt) was used in inhibition experiments. All kinetic studies were carried out at 25 °C and normal atmospheric pressure.

Slow-binding kinetic determination. To study the time dependence of inhibition of DHDPS by (*R*,*R*)-bislysine, experiments were performed by triggering the reaction by addition of DHDPS. Each progress curve was fit to eq 1,[15,16]

$$[P] = v_s t + \frac{v_z - v_s}{k_{obs}}(1 - e^{-k_{obs}t}) + d \quad (1)$$

where v_s and v_z are velocities at steady-state and at time zero, k_{obs} is the frequency constant of the exponential phase, t is time, d is displacement or finite intercept, and $[P]$ is related to the amount of product produced.

Steady-state kinetic studies. DHDPS was preincubated with the inhibitor (and other components of the assay) for 1 min and the reaction was initiated by addition of ASA. The concentration of one substrate was varied, while the concentration of the other was kept constant at saturating level (2.6 mM for ASA and 3.7 mM for pyruvate). All data points represent at least three experiments. The models for *mixed partial* (eq 2) and *noncompetitive partial* inhibition (eq 3) were used to fit experimental data with *SigmaPlot* 10.0 (Systat Software, San Jose, CA),

$$\frac{v}{V_{max}} = \frac{\frac{[S]}{K_s} + \frac{\beta[S][I]^h}{K_s(\alpha K_i)^h}}{1 + \frac{[S]}{K_s} + \frac{[I]^{h'}}{K_i^{h'}} + \frac{[S][I]^h}{K_s(\alpha K_i)^h}} \quad (2)$$

$$\frac{v}{V_{max}} = \frac{\frac{[S]}{K_s} + \frac{\beta[S][I]^h}{K_s K_i^h}}{1 + \frac{[S]}{K_s} + \frac{[I]^h}{K_i^h} + \frac{[S][I]^h}{K_s K_i^h}} \quad (3)$$

where V_{max} is the maximum velocity, K_S is the dissociation constant of the ES complex, v is the initial velocity. K_i is the inhibition constant, I is the inhibitor concentration, S is the substrate concentration, and α and β are proportionality constants. The cooperativity coefficients h' and h correspond to (*R*,*R*)-bislysine binding to E and E:pyr, respectively (eq 2). For eq 3, h is a cooperativity coefficient for (*R*,*R*)-bislysine binding to the F and F:ASA forms of the enzyme.

$$\log \frac{v_i - v_{i(sat)}}{v_0 - v_i} = \log K - h \log I \quad (4)$$

Equation 4 is the Hill equation for partial inhibition, where v_i is the velocity in the presence of the inhibitor, v_0 is the velocity in the absence of the inhibitor, $v_{i(sat)}$ is the reaction velocity at saturating concentrations of inhibitor, and K is an apparent overall dissociation constant.

X-ray crystallography of CjDHDPS:bislysine. Diffraction quality crystals were grown in a solution of 0.2 M sodium acetate, 16% P4000, 0.1 mM Tris pH 8.5 using the hanging drop vapor diffusion method. Protein and precipitant solutions where mixed in a 1:1 3 μL drop over

DOI: 10.1021/jacs.5b12695
J. Am. Chem. Soc. 2016, 138, 2014−2020

500 μL well. DHDPS was preincubated with 20 mM (±)-bisysine (tetrahydrochloride salt) prior to setting up crystallization trials. Crystals were transferred to a cryoprotectant solution consisting of 10% ethylene glycol, 30% PEG 400, 60% precipitant solution with 10 mM (±)-bisysine (tetrahydrochloride salt) and then flash-cooled in liquid nitrogen.

Diffraction experiments were conducted using synchrotron radiation at the Canadian Light Source (CLS) on the 08ID-01 beamlines using a wavelength of 0.9798 Å and equipped with a MAR CCD 300 area detector. Crystals were kept under a stream of liquid nitrogen and diffraction was carried out at 100 K. The images were integrated and scaled using auto-XDS/XSCALE[17] in-house at the CLS. Pertinent data collection statistics and refinement parameters are given in Supporting Information Table 1.

CjDHDPS:bislysine crystals were found to be space group $P2_12_12_1$. The structure was determined by molecular replacement using MOLREP[18] from the CCP4 suite using the solvent stripped wild type structure as the search model. The solution found four monomers organized as a tetramer in the asymmetric unit. Solvent content determined from Matthews coefficients[19] was 42.25%. Further refinements were made using PHENIX,[20] with manual model correction in COOT.[21] Structure quality was assessed using MOLPROBITY and validation tools in COOT. The final structure indicates that 98.5% of residues are in Ramachandran favored conformations, 1.5% are in acceptable conformations, and 0% in unacceptable conformations. Coordinates were deposited in the RSCB Protein Databank (PDB), code 5F1V.

X-ray crystallography of Y110F:bislysine. Diffraction quality crystals were grown in a solution of 0.28 M sodium acetate, 30% PEG 4000, 0.1 M TRIS pH 8.5 using the hanging drop vapor diffusion method. Protein and precipitant solutions where mixed in a 1:1 3 μL drop over 500 μL well. DHDPS was preincubated with 25 mM (±)-bisysine (tetrahydrochloride salt) prior to setting up crystallization trials. Crystals were transferred to a cryoprotectant solution consisting of 10% ethylene glycol, 30% PEG 400, 60% precipitant solution with 20 mM (±)-bisysine (tetrahydrochloride salt) and then flash-cooled in liquid nitrogen.

Diffraction experiments were conducted using synchrotron radiation at CLS on the 08ID-01 beamlines using a wavelength of 0.9795 Å and equipped with a MAR CCD 300 area detector. Crystals were kept under a stream of liquid nitrogen and diffraction was carried out at 100 K. The images were integrated and scaled using auto-XDS/XSCALE in-house at the CLS. Pertinent data collection statistics and refinement parameters are given in Supporting Infomation Table 1.

Y110F:bislysine crystals were found to be space group $P2_12_12_1$. The structure was determined by molecular replacement using MOLREP from the CCP4 suite using the solvent stripped wild type structure as the search model. The solution found four monomers organized as a tetramer in the asymmetric unit. Solvent content determined from Matthews coefficients was 40.49%. Further refinements were made using PHENIX, with manual model correction in COOT. Structure quality was assessed using MOLPROBITY and validation tools in COOT. The final structure indicates that 98.0% of residues are in Ramachandran favored conformations, 1.66% are in acceptable conformations, and 0.34% in unacceptable conformations. The coordinates were deposited as PDB code 5F1U.

RESULTS

Preparation of bislysine. Synthesis of the target inhibitor began by generation of the known Boc-protected methyl ester of 2,5-diaminoadipate from adipic acid in seven steps (Supporting Information). The key step in the synthesis was the alkylation of this product with 1-bromo-4-chlorobutane, as shown in Scheme 1. This was followed by introduction of the ε-amino groups using phthalimide, and acidic hydrolysis to form the final product. The alkylation proceeded in a moderate yield, but allowed alkylation of both α-carbon positions in a single step. This nonstereoselective approach yielded all three

Scheme 1[a]

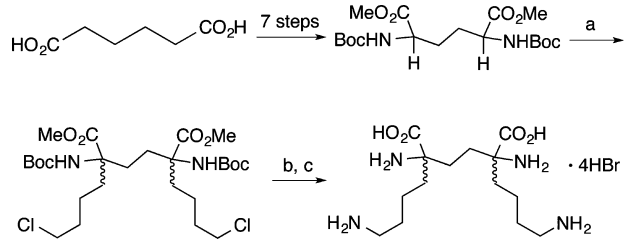

[a]Conditions: (a) 1-bromo-4-chlorobutane, LDA, THF/10% HMPA, −78 °C, 1 h, 16%. (b) potassium phthalimide, DMF, 90 °C, 2 h, 50%. (c) 1:1 48% HBr_{aq}:AcOH, 115 °C, 3 d; AG 50W-X2(H^+ form) eluted with HBr_{aq}, 88%.

stereoisomers: (*R*,*R*)-, (*S*,*S*)- and *meso*-bislysine. Before deprotection, the racemate was separated from the *meso*-compound by conventional flash chromatography. The pair of enantiomers can be resolved either before or after deprotection using chiral HPLC (Supporting Information), but the presence of the phthalimide groups allowed uv detection, which made separation for preparative purposes much more convenient. Deprotected compounds could be observed using evaporative light-scattering detection. Reinjection of purified (*R*,*R*)-bislysine showed that it contained no more than ∼2% of the (*S*,*S*)-isomer.

Inhibition. The desired (*R*,*R*)-enantiomer has the same relative configuration as a pair of L-lysine molecules. This enantiomer was an extremely effective inhibitor of *Cj*DHDPS, with an apparent IC_{50} ∼ 300 times lower than that of lysine (Figure 3). The other stereoisomers showed inhibition no greater than that consistent with contamination by traces of the active (*R*,*R*)-isomer.

As shown in the Supporting Information, the observed behavior was consistent with a slow-onset, one-step reversible inhibition mechanism. The analysis of progress curves (Supporting Information Figure 5) shows inhibition of DHDPS in a time-dependent manner, where equilibrium between the free inhibitor and enzyme species establishes within the first minute. The values of k_{obs} determined using eq 1 showed a linear relationship with inhibitor concentration, which suggested that a slow binding event, rather than fast binding followed by slow conversion to a tightly bound complex, occurs.[15] Values of the slope and intercept of this graph give values of k_{on} and k_{off} of $(4.4 \pm 1.2) \times 10^4$ M^{-1} s^{-1} and $(6.2 \pm 4.2) \times 10^{-3}$ s^{-1}, respectively. The ratio of these values gives an apparent K_i value of 140 nM, close to the observed IC_{50} value.

Steady-state kinetic analysis showed that the stronger binding of (*R*,*R*)-bislysine relative to lysine affected the kinetic mechanism of inhibition. Figure 4a shows the model for allosteric partial inhibition of a two-substrate enzymatic process. (*R*,*R*)-Bislysine is a mixed partial inhibitor with respect to pyruvate, and a noncompetitive partial inhibitor with respect to ASA as shown graphically in Figure 4b and 4c, respectively. These results are consistent with an inhibitor that binds to the allosteric site regardless of the presence of pyruvate, whereas our previous results showed that lysine, an uncompetitive partial inhibitor, does not bind to apoenzyme (or not in a way that affects the reaction).[5] Table 1 shows the inhibition constants and Hill coefficients calculated using eqs 2, 3, and 4. Our results show that bislysine binds to all forms of the enzyme with a K_i near 200 nM, by far the lowest value ever observed for

DOI: 10.1021/jacs.5b12695
J. Am. Chem. Soc. 2016, 138, 2014−2020

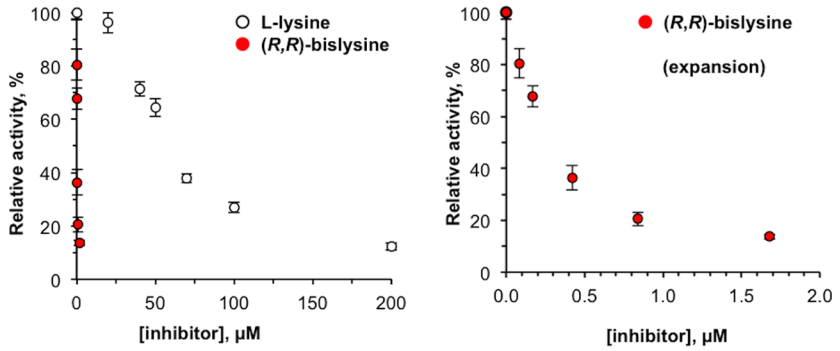

Figure 3. L-Lysine and (*R,R*)-bislysine inhibition of DHDPS activity at 0.16 mM ASA and 3.5 mM pyruvate (left), and an expansion of the same plot (right).

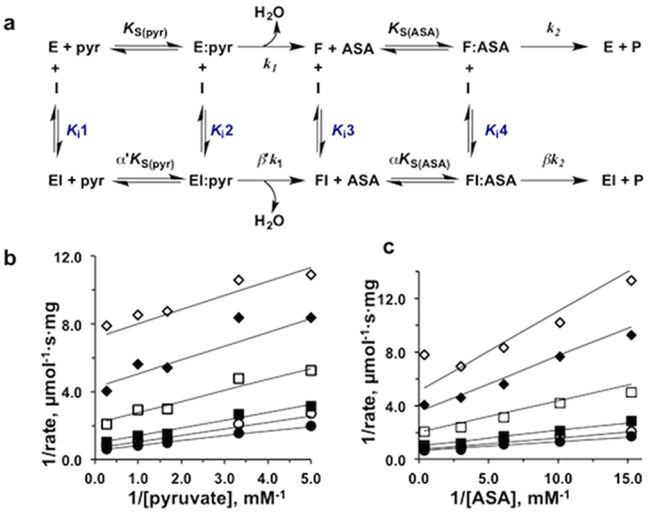

Figure 4. (*R,R*)-Bislysine inhibition of DHDPS. (a) General scheme of (*R,R*)-bislysine inhibition, α (and α') must be >0, while β (and β') must be <1 for inhibition. In a pure noncompetitive partial inhibition mechanism, α and $\alpha' = 1$; therefore, $K_i1 = K_i2$, $K_i3 = K_i4$, whereas in a mixed partial inhibition mechanism, α and $\alpha' \neq 1$ ($K_i1 \neq K_i2$, $K_i3 \neq K_i4$). (b) Lineweaver–Burk plot of data obtained at a constant ASA concentration of 2.6 mM. Concentration of (*R,R*)-bislysine: (●) 0 μM, (○) 0.084 μM, (■) 0.17 μM, (□) 0.42 μM, (◆) 0.84 μM, (◇) 1.7 μM. Solid lines are fit lines, obtained by globally fitting the *mixed partial* model (R^2 = 0.98) to the data. Residuals are shown in Supporting Information Figure 9. (c) Lineweaver–Burk plot of data obtained at a constant pyruvate concentration of 3.7 mM. Concentration of (*R,R*)-bislysine: (●) 0 μM, (○) 0.084 μM, (■) 0.17 μM, (□) 0.42 μM, (◆) 0.84 μM, (◇) 1.7 μM. Solid lines are fit lines, obtained by globally fitting the *noncompetitive partial* model (R^2 = 0.99) to the data. Residuals are shown in Supporting Information Figure 10.

inhibition of DHDPS. Tellingly, bislysine inhibition is also cooperative (h = 1.6–1.7), in concert with our prior observation that the antipodal allosteric sites do not behave independently. It is clear that occupancy of the allosteric site has a global effect on the tetrameric protein.

X-ray crystallography. We crystallized *Cj*DHDPS in the presence of a racemic mixture of (*R,R*)- and (*S,S*)-bislysine, and determined the structure to 2.2 Å resolution. As with previous structures of *Cj*DHDPS,[14] the electron density difference map showed clear positive density within the active site consistent with the Schiff-base formed by Lys166 and pyruvate. The resulting structure showed that bislysine was unambiguously present in the allosteric site, and that the (*R,R*)-enantiomer had

Table 1. Hill Coefficients and Inhibition Constants (as defined in Figure 4) DHDPS Inhibition by Bislysine

	Pyruvate[a]	ASA[b]
h_E	1.0 ± 0.2	
$h_{E:pyr}$	1.6 ± 0.1	
h_F		1.7 ± 0.1
$h_{F:ASA}$		1.7 ± 0.1
K_i1, nM	240 ± 50	
K_i2, nM	170 ± 70	
K_i3, nM		200 ± 20
K_i4, nM		200 ± 20

[a]Fit to the mixed partial inhibition kinetic model (eq 2). [b]Fit to a noncompetitive partial inhibition kinetic model (eq 3).

been selectively complexed from solution. The tetramer complexed with two molecules of bislysine is shown in Figure 5A, and the omit map of one allosteric site is shown in Figure 5B. Figure 5C shows the equivalent binding mode of (*R,R*)-bislysine and L-lysine in the allosteric site.

We previously observed that binding of lysine to *Cj*DHDPS results in changes to the volume of both the allosteric and active sites of the enzyme, revealing one of the mechanisms by which lysine can affect catalysis without making large-scale changes to the protein structure. Specifically, lysine binding to *Cj*DHDPS reduces the volume of the allosteric site by 43% (ignoring the contribution by lysine) and increases the volume of the active site by 22%.[14] When we repeated this analysis using our bislysine-bound structure, we saw that these effects were similar, even enhanced: the allosteric site volume decreases by 49% upon binding of bislysine, while the active-site volume increases by 34%.

Allosteric site mutant Y110F. We recently showed that Tyr110, a residue within the allosteric site which forms a hydrogen bond with the carboxylate group of a bound lysine molecule, was critical for effective inhibition by lysine.[14] Tyr110 is adjacent to Tyr111, a residue which is part of an apparent catalytic triad that is integral to catalysis. Mutation of Tyr110 to phenylalanine removes the hydroxyl group responsible for this hydrogen bond, just one of the many polar interactions between the inhibitor and the protein. The mutant Y110F has a turnover number reduced by half, but is nearly insensitive to inhibition by lysine, with an estimated IC_{50} > 40 mM. A crystal structure of Y110F bound to lysine showed that the loss of this hydrogen bond resulted in dissipation of several effects of lysine binding observed in the wild-type enzyme.[14] In particular, the binding of lysine to Y110F reduces the volume of the allosteric site by only 26%, considerably less than the 43% observed with

DOI: 10.1021/jacs.5b12695
J. Am. Chem. Soc. 2016, 138, 2014–2020

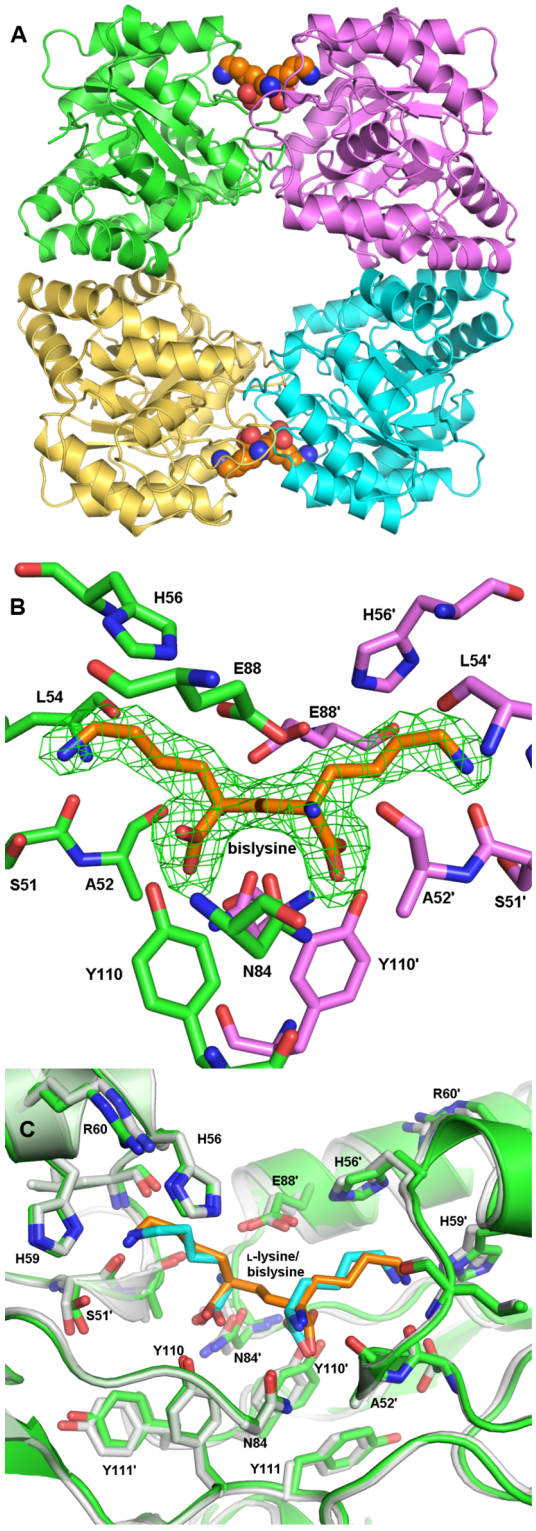

Figure 5. Crystal structure of *Cj*DHDPS with (*R*,*R*)-bislysine bound at the allosteric site. (A) (*R*,*R*)-bislysine (orange) bound at the allosteric site of wild-type *Cj*DHDPS (PDB 5F1V). Residues of monomers A and B are shown in green and yellow, respectively. (B) Electron density of bislysine bound to the allosteric site of DHDPS. The green mesh is the electron density omit map scaled at 3σ. Monomer A is green, monomer B (primed residues) is magenta. (C) Overlay of crystal structures of (*R*,*R*)-bislysine (orange inhibitor, green protein) and L-lysine (cyan inhibitor, white protein, PDB code 4M19) bound at the allosteric site of *Cj*DHDPS.

wild-type enzyme. Similarly, while lysine binding to wild-type increases the volume of the active site by 22%, in the Y110F mutant the active site shows a slight *decrease* in volume. These results suggest that a drug targeting the allosteric site of DHDPS might be prone to resistance, since a single mutation can result in a functioning catalyst that is insensitive to inhibition. However, (*R*,*R*)-bislysine is a very potent inhibitor of Y110F, with an IC_{50} of 400 nM (Supporting Information), indicating that (*R*,*R*)-bislysine inhibits this mutant nearly as well as it does wild-type, and 10^5 times more effectively than L-lysine. Clearly the advantages of the bislysine design, the occupancy of the entire allosteric site by a single molecule, outweigh the effects of that hydrogen bond. We crystallized Y110F in the presence of bislysine, and the resulting structure closely resembles that of wild-type DHDPS bound to inhibitor. Changes in cavity volumes in the Y110F-bislysine structure are consistent with the trend shown for lysine and bislysine complexation with wild-type *Cj*DHDPS; that is, the volume of the allosteric site of Y110F decreases by 38% upon bislysine binding, while the volume of the active site increases by 16%.

DISCUSSION

Several reports show that DHDPS is a potential target for drug development;[22] *Escherichia coli* AT997 (a mutant strain lacking the DHDPS-encoding gene *dapA*) can be maintained on nutrient medium only if the medium is supplemented with diaminopimelate,[2,23,24] and *dapA* was classified as "essential" for *Bacillus subtilis*[25] and *Haemophilus influenzae*.[26] (This is not universally the case, however: Schnell et al. showed that *Pseudomonas aeruginosa* mutants lacking *dapA* are viable.[27]) The therapeutic potential has inspired the design of DHDPS inhibitors, but effective inhibition has proved elusive. Efforts have concentrated on the active site, resulting in millimolar-range inhibitors including analogs of substrates pyruvate and ASA,[28−30] analogs of product HTPA or DHDP,[6,7,29−33] and mimics of enzyme-bound condensation products of ASA and pyruvate.[7−9,34] Targeting of the active site is the common approach to rational design, since one typically has specific information about the molecules that fit that site. There are many examples of successful inhibitors which appear to capture the binding energy associated with recognition of the transition state, such as Schramm's femtomolar inhibitors of methylthioadenosine nucleosidase.[35] In the case of DHDPS, however, the precise binding location and conformation of the natural regulator lysine is available, providing a natural template for developing new inhibitors. We sought to establish that the allosteric site can be targeted effectively, which might open a new avenue to drug design.

Bislysine proved to be a very effective inhibitor, and the crystal structure of (*R*,*R*)-bislysine bound to the allosteric site shows how closely it mimics the binding of two (*S*)-lysine molecules. The slow-onset character of the inhibition may be due to the fact that bislysine binds to a site designed for egress of a pair of smaller molecules. The X-ray structure shows that amino acid side chains, His56 (and His56′) in particular, would need to move to allow bislysine to bind (Figure 5b and 5c). This necessary movement is the most likely explanation, given that there has been no observation of an "open and closed conformation" or similar significant conformational change.

We believed that the design of a single molecule to occupy the entire allosteric site would be an effective inhibition strategy, a concept often seen in the design of "bisubstrate analog" inhibitors. Such ligands can make many specific

DOI: 10.1021/jacs.5b12695
J. Am. Chem. Soc. 2016, 138, 2014−2020

interactions with the protein, resulting in higher affinity and enhanced selectivity. However, we did not predict that bislysine would be such an effective inhibitor of the Y110F mutant. The very weak inhibition of this mutant observed in the presence of lysine led us to believe that the presence of a tyrosine residue in this position was crucial to inhibition. Instead, bislysine is nearly as effective an inhibitor of Y110F as of the wild-type DHDPS. The result underscores that our view was overly reductionist, and that multiple mechanisms may be used simultaneously to effect inhibition.

Allosteric inhibition is often characterized by very noticeable changes in the shape of the enzyme. In the case of DHDPS, however, the changes in shape are not immediately obvious. As we have discussed previously,[14] binding of lysine to DHDPS results in small domain movements, effectively rotating the portion of the $(\beta/\alpha)_8$ barrel that includes β-strands 4, 5, and 6 relative to the rest of the barrel by just under 4 degrees. This subtle movement results in an increased volume of the active site, and a decreased volume of the allosteric site. Any expectation that the inhibitor has disrupted the active site is not borne out. The key residues of the active site include K166, which forms the crucial Schiff base with pyruvate, and the "catalytic triad" of Y137, T47, and Y111′. The relative positions of these residues in the crystal do change when lysine is bound to the allosteric site, but none by more than about 0.5 Å. Even assuming that these changes reflect a difference in the conformation of the enzyme in solution, it is difficult to estimate the extent to which such changes affect catalysis. Lysine's effects on the TIM barrel also result in small but significant changes at the weak dimer−dimer interface, specifically between residues found on helices 6, 7, and 8 (see Supporting Information, Figure 14). The bislysine-bound DHDPS structure shows similar changes, and the cooperativity observed for inhibition by bislysine, despite binding sites being separated by over 50 Å, may be a manifestation of these alterations in dimer−dimer interactions. It is noteworthy that the structure of Y110F bound to lysine does not show these changes relative to the unliganded structure, but bislysine-bound Y110F does. The additional contacts to both monomer surfaces within the allosteric site apparently overcome the loss of interaction with Y110. It is clear that the summation of many small effects upon the protein result in inhibition.

CONCLUSION

Biomimetic design based on the X-ray crystal structure of lysine molecules bound to the allosteric site of *Cj*DHDPS resulted in a very potent inhibitor, one whose design appears to protect it from simple mutational resistance. The bis-inhibitor approach clearly demonstrates how a single molecule that binds to two sites (in this case two binding sites within a single allosteric cavity) can be more effective than two molecules. The observed cooperativity of (*R*,*R*)-bislysine verifies that inhibition is achieved in part by structural effects across the tetrameric enzyme. By demonstrating that this enzyme is susceptible to potent inhibitors, we believe the dap pathway remains a viable target for novel antibiotic research.

ASSOCIATED CONTENT

Supporting Information

The Supporting Information is available free of charge on the ACS Publications website at DOI: 10.1021/jacs.5b12695.

Synthetic methods, supplementary kinetic methods, X-ray crystallography statistics, and NMR spectra. (PDF)

AUTHOR INFORMATION

Corresponding Authors

*david.sanders@usask.ca

*dave.palmer@usask.ca

Notes

The authors declare no competing financial interest.

ACKNOWLEDGMENTS

This work was supported by NSERC Discovery Grants to D.R.J.P. and D.A.R.S., and NSERC PGS awards to Y.V.S. and C.J.T.C. The authors thank Keith Brown, Ken Thoms, and other staff of the Saskatchewan Structural Sciences Centre. The protein crystallographic studies described in this paper were performed at the CLS, which is supported by NSERC, the National Research Council of Canada, the Canadian Institutes of Health Research, the Province of Saskatchewan, Western Economic Diversification Canada, and the University of Saskatchewan.

REFERENCES

(1) Lee, J. H.; Jeong, S. H.; Cha, S.-S.; Lee, S. H. *Nat. Rev. Drug Discov.* **2007**, *6*, DOI: 10.1038/nrd2201-c1031.

(2) Bukhari, A. I.; Taylor, A. L. *J. Bacteriol.* **1971**, *105*, 844.

(3) Dogovski, C.; Gorman, M. A.; Ketaren, N. E.; Praszkier, J.; Zammit, L. M.; Mertens, H. D.; Bryant, G.; Yang, J.; Griffin, M. D. W.; Pearce, F. G.; Gerrard, J. A.; Jameson, G. B.; Parker, M. W.; Robins-Browne, R. M.; Perugini, M. A. *Plos One* **2013**, *8*, DOI: 10.1371/journal.pone.0083419.

(4) Blickling, S.; Renner, C.; Laber, B.; Pohlenz, H. D.; Holak, T. A.; Huber, R. *Biochemistry* **1997**, *36*, 24.

(5) Skovpen, Y. V.; Palmer, D. R. J. *Biochemistry* **2013**, *52*, 5454.

(6) Turner, J. J.; Gerrard, J. A.; Hutton, C. A. *Bioorg. Med. Chem.* **2005**, *13*, 2133.

(7) Turner, J. J.; Healy, J. P.; Dobson, R. C. J.; Gerrard, J. A.; Hutton, C. A. *Bioorg. Med. Chem. Lett.* **2005**, *15*, 995.

(8) Boughton, B. A.; Griffin, M. D. W.; O'Donnell, P. A.; Dobson, R. C. J.; Perugini, M. A.; Gerrard, J. A.; Hutton, C. A. *Bioorg. Med. Chem.* **2008**, *16*, 9975.

(9) Boughton, B. A.; Hor, L.; Gerrard, J. A.; Hutton, C. A. *Bioorg. Med. Chem.* **2012**, *20*, 2419.

(10) Phenix, C. P.; Palmer, D. R. J. *Biochemistry* **2008**, *47*, 7779.

(11) Muscroft-Taylor, A. C.; Soares da Costa, T. P.; Gerrard, J. A. *Biochimie* **2010**, *92*, 254.

(12) Voss, J. E.; Scally, S. W.; Taylor, N. L.; Atkinson, S. C.; Griffin, M. D. W.; Hutton, C. A.; Parker, M. W.; Alderton, M. R.; Gerrard, J. A.; Dobson, R. C. J.; Dogovski, C.; Perugini, M. A. *J. Biol. Chem.* **2010**, *285*, 5188.

(13) Atkinson, S.; Dogovski, C.; Downton, M.; Czabotar, P.; Dobson, R. J.; Gerrard, J.; Wagner, J.; Perugini, M. *Plant Mol. Biol.* **2013**, *81*, 431.

(14) Conly, C. J. T.; Skovpen, Y. V.; Li, S.; Palmer, D. R. J.; Sanders, D. A. R. *Biochemistry* **2014**, *53*, 7396.

(15) Morrison, J. F.; Walsh, C. T. *Adv. Enzymol. Relat. Areas Mol. Biol.*; John Wiley & Sons, Inc.: 1988, p 201.

(16) Frieden, C. *J. Biol. Chem.* **1970**, *245*, 5788.

(17) Kabsch, W. *Acta Crystallogr., Sect. D: Biol. Crystallogr.* **2010**, *66*, 125.

(18) Vagin, A.; Teplyakov, A. *Acta Crystallogr., Sect. D: Biol. Crystallogr.* **2010**, *66*, 22.

(19) Matthews, B. W. *J. Mol. Biol.* **1968**, *33*, 491.

(20) Adams, P. D.; Afonine, P. V.; Bunkoczi, G.; Chen, V. B.; Davis, I. W.; Echols, N.; Headd, J. J.; Hung, L.-W.; Kapral, G. J.; Grosse-Kunstleve, R. W.; McCoy, A. J.; Moriarty, N. W.; Oeffner, R.; Read, R.

DOI: 10.1021/jacs.5b12695
J. Am. Chem. Soc. 2016, 138, 2014−2020

J.; Richardson, D. C.; Richardson, J. S.; Terwilliger, T. C.; Zwart, P. H. *Acta Crystallogr., Sect. D: Biol. Crystallogr.* **2010**, *66*, 213.
(21) Emsley, P.; Cowtan, K. *Acta Crystallogr., Sect. D: Biol. Crystallogr.* **2004**, *60*, 2126.
(22) Hutton, C. A.; Perugini, M. A.; Gerrard, J. A. *Mol. BioSyst.* **2007**, *3*, 458.
(23) Yeh, P.; Sicard, A. M.; Sinskey, A. J. *Mol. Gen. Genet.* **1988**, *212*, 105.
(24) Neidhardt, F. C.; Curtiss, R. *Escherichia coli and Salmonella: cellular and molecular biology*, 2nd ed.; ASM Press: Washington, D.C., 1996.
(25) Kobayashi, K.; Ehrlich, S. D.; Albertini, A.; Amati, G.; Andersen, K. K.; Arnaud, M.; Asai, K.; Ashikaga, S.; Aymerich, S.; Bessieres, P.; Boland, F.; Brignell, S. C.; Bron, S.; Bunai, K.; Chapuis, J.; Christiansen, L. C.; Danchin, A.; Debarbouille, M.; Dervyn, E.; Deuerling, E.; Devine, K.; Devine, S. K.; Dreesen, O.; Errington, J.; Fillinger, S.; Foster, S. J.; Fujita, Y.; Galizzi, A.; Gardan, R.; Eschevins, C.; Fukushima, T.; Haga, K.; Harwood, C. R.; Hecker, M.; Hosoya, D.; Hullo, M. F.; Kakeshita, H.; Karamata, D.; Kasahara, Y.; Kawamura, F.; Koga, K.; Koski, P.; Kuwana, R.; Imamura, D.; Ishimaru, M.; Ishikawa, S.; Ishio, I.; Le Coq, D.; Masson, A.; Mauel, C.; Meima, R.; Mellado, R. P.; Moir, A.; Moriya, S.; Nagakawa, E.; Nanamiya, H.; Nakai, S.; Nygaard, P.; Ogura, M.; Ohanan, T.; O'Reilly, M.; O'Rourke, M.; Pragai, Z.; Pooley, H. M.; Rapoport, G.; Rawlins, J. P.; Rivas, L. A.; Rivolta, C.; Sadaie, A.; Sadaie, Y.; Sarvas, M.; Sato, T.; Saxild, H. H.; Scanlan, E.; Schumann, W.; Seegers, J. F.; Sekiguchi, J.; Sekowska, A.; Seror, S. J.; Simon, M.; Stragier, P.; Studer, R.; Takamatsu, H.; Tanaka, T.; Takeuchi, M.; Thomaides, H. B.; Vagner, V.; van Dijl, J. M.; Watabe, K.; Wipat, A.; Yamamoto, H.; Yamamoto, M.; Yamamoto, Y.; Yamane, K.; Yata, K.; Yoshida, K.; Yoshikawa, H.; Zuber, U.; Ogasawara, N. *Proc. Natl. Acad. Sci. U. S. A.* **2003**, *100*, 4678.
(26) Akerley, B. J.; Rubin, E. J.; Novick, V. L.; Amaya, K.; Judson, N.; Mekalanos, J. J. *Proc. Natl. Acad. Sci. U. S. A.* **2002**, *99*, 966.
(27) Schnell, R.; Oehlmann, W.; Sandalova, T.; Braun, Y.; Huck, C.; Maringer, M.; Singh, M.; Schneider, G. *Plos One* **2012**, *7*, DOI: 10.1371/journal.pone.0031133.
(28) Coulter, C. V.; Gerrard, J. A.; Kraunsoe, J. A. E.; Moore, D. J.; Pratt, A. J. *Tetrahedron* **1996**, *52*, 7127.
(29) Hutton, C. A.; Southwood, T. J.; Turner, J. J. *Mini-Rev. Med. Chem.* **2003**, *3*, 115.
(30) Coulter, C. V.; Gerrard, J. A.; Kraunsoe, J. A. E.; Pratt, A. J. *Pestic. Sci.* **1999**, *55*, 887.
(31) Couper, L.; Mckendrick, J. E.; Robins, D. J.; Chrystal, E. J. T. *Bioorg. Med. Chem. Lett.* **1994**, *4*, 2267.
(32) Walters, D. R.; McPherson, A.; Robins, D. J. *Mycol. Res.* **1997**, *101*, 329.
(33) Mitsakos, V.; Dobson, R. C. J.; Pearce, F. G.; Devenish, S. R.; Evans, G. L.; Burgess, B. R.; Perugini, M. A.; Gerrard, J. A.; Hutton, C. A. *Bioorg. Med. Chem. Lett.* **2008**, *18*, 842.
(34) Boughton, B. A.; Dobson, R. C.; Gerrard, J. A.; Hutton, C. A. *Bioorg. Med. Chem. Lett.* **2008**, *18*, 460.
(35) Singh, V.; Evans, G. B.; Lenz, D. H.; Mason, J. M.; Clinch, K.; Mee, S.; Painter, G. F.; Tyler, P. C.; Furneaux, R. H.; Lee, J. E.; Howell, P. L.; Schramm, V. L. *J. Biol. Chem.* **2005**, *280*, 18265.

DOI: 10.1021/jacs.5b12695
J. Am. Chem. Soc. 2016, 138, 2014−2020